JOURNAL LA MULTIAPP

VOL. 02, ISSUE 02 (010-030), 2021
DOI: 10.37899/journallamultiapp.v2i2.339

Fault Diagnostic Methodology for Grid-Connected Photovoltaic Systems

Proenza Y. Roger[1], Camejo C. José Emilio[1], Ramos H. Rubén[1]

[1]*Solar Energy Research Center, Reparto Abel Santamaría, Micro 3, Santiago de Cuba, Cuba*

**Corresponding Author: Proenza Y. Roger*

Article Info

Article history:
Received 19 March 2021
Received in revised form 13 April 2021
Accepted 25 April 2021

Keywords:
Faults
Diagnosis
Estimation and Accommodation
Photovoltaic systems
Monitoring and Supervision

Abstract

This research focuses on the design of a fault diagnosis methodology to contribute to the improvement of efficiency, maintainability and availability indicators of Grid-Connected Photovoltaic Systems. To achieve this, we start from the study of the mathematical model of the photovoltaic generator, then, a procedure is performed to quantify the operational losses of the photovoltaic generator and adjust the mathematical model of this to the real conditions of the system, through a polynomial adjustment. A real system of nominal power 7.5 kWp installed in the Solar Energy Research Center of the province of Santiago de Cuba is used to evaluate the proposed methodology. Based on the results obtained, the proposed approach is validated to demonstrate that it successfully supervises the system. The methodology was able to detect and identify 100% of the simulated failures and the tests carried out had a maximum false alarm rate of 0.22%, evidencing its capacity.

Introduction

Electricity generation has been one of the main challenges that humanity has faced, with the absence of this socio-economic systems would not develop. It is a fact that fossil resources are limited and given the growth of global energy demand, they are expected to run out within a few years. In addition, the increasing and continuous use of primary energies has caused great damage to the environment, problems such as global warming and melting of the poles are consequences of their use. One of the alternatives of electricity generation, friendly to the environment, are the Renewable Energy Sources (SRE), an alternative that in 2008 was very poor in terms of its introduction and use in Cuba, but with the actions that are coming by 2030 electricity generation from SRE is expected to cover 24% of national demand (Gutiérrez et al., 2018) see Figure 1.

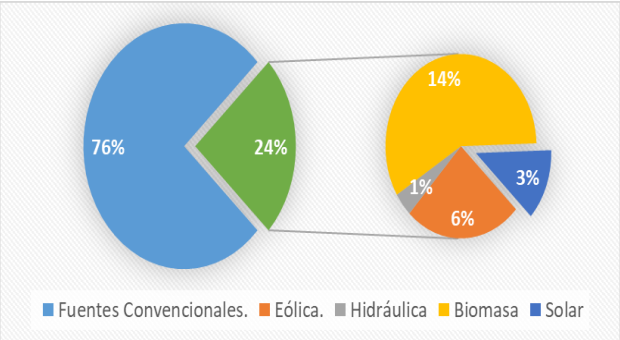

Figure 1. Planning of electricity generation from SRE by 2030

ISSN: 2716-3865 (Print), 2721-1290 (Online)

Among the alternatives for electricity generation, one of the most widespread currently are Grid-Connected Photovoltaic Systems (SPVGC). The high and stable potential of solar radiation in the field occupied by the Solar Energy Research Center, Santiago de Cuba (SERC) throughout the year means that this index is around 5 kW-h/m2 daily adaptability of technology to local conditions favor its introduction. Currently, one of the objectives pursued by research groups and industry in this sector is to improve the performance of installed Photovoltaic Systems (SPV), i.e. to increase electricity production by reducing losses, that the systems are comply with safety measures (Villegas Berbesi, 2012). Under practical conditions, failures that are unavoidable in SPV, can result in power loss, partial or total system disconnection, and even serious security breaches (Brooks, 2011).

Detection of these in SPV is therefore crucial to maintaining normal operations by providing early failure warnings. In fact, accurate and early detection of failures in a photovoltaic system is critical to prevent its progression and significantly reduce productivity losses (Garoudja et al., 2017). Several Failure Diagnostics (DDF) techniques have been developed for SPV, dividing these into two large groups: process history-based approaches (Mekki et al., 2016) and model-based approaches (Chouder and Silvestre, 2010), (Vergura et al., 2009), (Chouder and Silvestre, 2009), achieving good results in the detection and early identification of system-level failures, mainly on the DC side. The current restrictions of these techniques are aimed at the ability to determine the number of elements that are fault conditioned, i.e. number of PV modules or chains of PV modules, which leads to insufficient diagnosis that serves as a to take actions that enable the management of greater efficiency. The main contribution of this work is aimed at the development of a model-based DDF methodology, which allows not only the detection and classification of the type of failure that occurs on the direct current (DC) side in an SPVGC, but also to the determination of the number of modules or chain modules, which are in a condition of failure. Another contribution provided by this work is the development of a procedure to quantify the operational losses of the GPV, which allows to have an accurate knowledge of the degradation status of the GPV, allowing to take maintenance actions to conserve SPVGC under nominal operating conditions.

The rest of this document is organized as follows. Section 2, provides a brief description of the SPVGC that provided data for this study and analysis of potential failures and losses. In Section 3, the basis of the proposed methodology is created when reviewing the mathematical model of the GPV, in this case the 5-parameter model popularized by (De Soto et al., 2006). Section 4 designs and implements a procedure for determining SPVGC operational losses. Section 5 develops a DDF strategy for the SPVGC and evaluates the proposed strategy in a real system installed in the SERC. Finally, Section 6 details the conclusions according to the results obtained.

SPVGC de 7.5 kWp installed in the SERC.

The SPVGC, used as part of this research, in which the proposed methodology is implemented, is located in the Abel Santamaria Cast, Micro 3, Santiago de Cuba municipality, province of the same name, located in the central part of the land occupied by SERC. It is located in the coordinates, Latitude: 20o 00o 75" and Longitude: 75o 77o 07".

In 2016, the SERC of Santiago de Cuba, carried out a project linked to the national program of Renewable Energy Sources called: “Evaluation of the Santiago Photovoltaic Park - 2.5 MW SERC grid -connected to the National Electricity”, which had as its main objective to

ISSN: 2716-3865 (Print), 2721-1290 (Online)

know the performance in the operation of this, since its implementation the technology had not been evaluated. Completion of the study yielded the following results:

There is a power deviation of the Photovoltaic Generator (GPV), table 1, lower than the nominal value given by the manufacturer, indicating that, for this reason, the system ceases to produce in a month approximately 23.81 MW.

Table 1. Average power measured relative to the number of modules for Standard Measurement Conditions (STC).

	Group 1	Group 2	Group 3	Group 4	Group 5	Group 6
Average power measured *(Wp)*	231.96	226.92	224.23	222.19	219.19	212.95
Number of modules	1	8	28	30	27	7
% of total modules	1	7.92	27.72	29.70	26.73	6.93
Average deviation (%)	-3.35	-5.45	-6.57	-7.42	-8.67	-11.27

• It is estimated that in 2016 the Santiago SERC Photovoltaic Park (PPV) operated at 91% of its nominal yield, Figure 2, so the operating losses of the system generally amount to 25.2 MW.h per month.

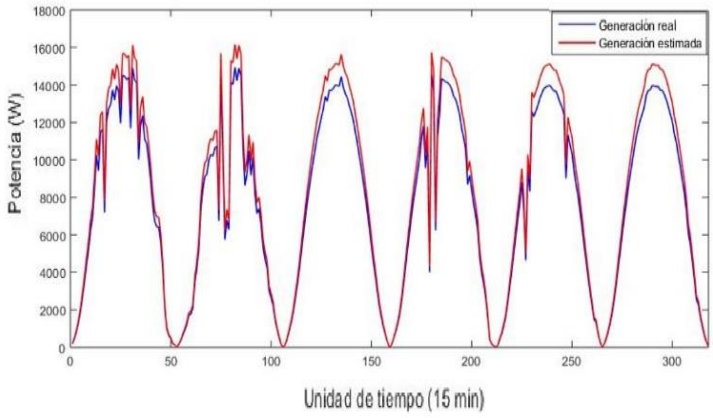

Figure 2. Power behavior generated and estimated for 6 days from one of the inverters installed in the PPV Santiago SERC, model SMA 17000TL.

The results of this study underpin the need to improve system indicators and reduce losses by leveraging existing technology. However, even though PPVs have an associated system Supervisory Control and Data Adquisition (SCADA), this only allows the monitoring of the installation, i.e. the real-time recording of the process variables, say, voltage and direct current and alternating current (AC), as well as the active power at the output of the inverter and the environmental variables (irradiance and operating temperature of the PV module), but does not allow monitoring of it, that is, the processing of that information to detect deviations that take the system away from an acceptable state of operation, and according to this, make a diagnosis.

Limitations of the SCADA of the PPV Santiago SERC: (1) Does not provide information about failures occurring at the PV module level. Each 250 Wp PV module generates approximately 1,050 kWh /day, a fault in this component is imperceptible on the part of the operator, so losses from this concept are present for long periods of time. (2) There is no real-time evaluation of the performance of the main elements that make up the system, say GFV and grid- connection inverter (IGC), making it difficult to manage efficiency in operation, maintenance and false expectations in planning energy production. (3) SCADA has no tool

ISSN: 2716-3865 (Print), 2721-1290 (Online)

for managing historical failure information, hindering feasibility studies for the technical quality of PPVs.

In general, the SCADA that accompanies the monitoring of the Santiago - SERC PPV, is not provided with systems that allow it to diagnose, detect, isolate and correct faults, so much of the fault detection is carried out by the operators, that is, in a way which implies inefficiencies in this process given the subjective decisions to which these diagnoses are subjected. Therefore, it is necessary to create a loss management procedure and a fault diagnostic system to improve system quality indicators. This requires deepening existing technology.

Photovoltaic Generator

The GFV, Figure 3, is composed entirely of 30 PV modules, rated power 250 Wp, model HELIENE215MA, table 2, grouped into three worktables consisting of three chains of 10 modules, each with a power of 2.5 kWp, 303 VDC and 8.22 A, which in its entirety has a rated power of 7.5 kWp

Figure 3: Photovoltaic Generator 7.5 kWp.

Power conditioning unit. Inverter

One of the fundamental devices of an SPVGC is the Inverter, which acts as an interface between the GPV and the electrical grid. In this way, the SPVGC is part of the generation systems that power that grid. The system is formed, on the AC side by two Inverters Model FRONIUS 5000k, Figure 4, connected one to two chains of 10 PV modules, and another to a chain of the same number of PV modules. These inverters follow the frequency to the corresponding voltage of the network to which they are connected, the waveform of the inverter output current is sinusoidal, minimizing the content of harmonics injected into the grid.

Figure 4. FRONIUS PRIMO Grid- Connection Photovoltaic Inverter

ISSN: 2716-3865 (Print), 2721-1290 (Online)

The main features of this inverter are: maximum DC power of 5000 W, nominal DC voltage of 660 V, maximum DC current equal to 18 A, working frequency 50 Hz and 60 Hz, maximum AC power of 5000 W, AC voltage range between 194-242 V and max current AC of 22.7 A.

The inverter at the input allows to measure up to a maximum of 1000 V and 10 A, with an accuracy of 2 %. These are internally provided with protections, both in the DC input with varistors for over-voltages and at the AC outlet with fuses and a grounding.

FRONIUS Data Acquisition System

The FRONIUS technology has a data management system, called Fronius Datamanager, that allows the monitoring of the installation in real time through a WEB server, providing the user with the necessary information of energy production, as well as like other system parameters as a whole. The system is capable of monitoring both environmental variables: irradiance and operating temperature of the PV module, as well as electrical variables: voltage and current of the GPV at the Maximum Power Point (PMP), voltage and alternating current as well as the effective power at the investor's exit. All these measurements are made every 5 minutes and form an operation database that is updated by the Fronius Solar Access Software, Figure 5, and that allows, among other functionalities, the export of the data to Excel.

Figure 5. Fronius Solar Access Database Manager Software.

Based on this technology, the loss assessment and fault detection system must be created. Therefore, it is necessary to know the approaches to losses and failures in SPVGC that are used internationally.

Approaches to SPVGC fault diagnosis

There are two categories for classifying energy losses that occur in an SPV: operational losses and failures (Firth, 2006). The former, inherent in any photovoltaic system, are associated with the inconsistency between the nominal efficiency declared by the manufacturer and the actual, the resistive energy losses in the cables or losses due to component degradation. On the other hand, failures are associated with malfunction or an unexpected change in the behavior of at least one system component. A basic approach to detecting failures in an SPVGC is to compare the power output of the GPV with a reference value and trigger an alarm when large differences are detected. The approach adopted in (Stettler et al., 2005) is to carry out monitoring using satellites, essentially obtaining known weather conditions.

Meyer & Van Dyk, (2004) describes an active approach, which studies the I-V curve to detect faults and records over time the point of maximum voltage and current power. Due to the nature of the sweep of I-V curves there is a reduction in output power during the analysis, i.e. it is not applicable to passive system studies. Two studies (Vergura et al., 2009), (Vergura et al., 2008) consider several identical photovoltaic chains and compare the outputs to classify significant deviations. This is done by checking whether certain statistical assumptions can be made, formally the output power differences of the GPV are

ISSN: 2716-3865 (Print), 2721-1290 (Online)

distributed independently with equal variance. If this is the case, a method known as variance analysis can be applied (Vergura et al., 2009) to build a confidence interval for the power output of each photovoltaic array (PV).

Another statistical approach takes it (Zhao et al., 2013) which involves a set of identical PV chains and attempts to classify the deviations from one from the other. This is done by building confidence intervals using different methods: 3 Sigma rule, Hampel identifier, among others. In the case of knowledge that surrounds the faults, it is possible to apply supervised learning, (Zhao et al., 2012), where a set of labeled data containing manually classified measures is available. This data set can be generated, for example, by measuring the voltage and current of the PV modules operating under fault conditions. The document analyzes a decision tree model that takes the available actions and places most of the dataset based on a likely classification. The study concludes that classification performance is very good, but real-life applications are limited because the dataset is closely linked to a specific PV facility.

Most methods focus on a specific parameter and do not seek the interrelationship between several of them, nor on the nature of the causes. This is why it delves into typical failures to create a procedure that can detect their causes based on their consequences.

Typical failures in SPVGC

It can be said that there is a wide range of failure conditions that occur on the DC side in SPVGC (Munoz et al., 2011), (Houssein et al., 2010). This wide range motivates the use of fault classification based on electrical properties induced during a failure (Zhao, 2010) and uses a categorization in open circuit failures and short-circuit failures (Zhao et al., 2013), (Zhao et al., 2014). Short circuit failures occur when two different potentials are accidentally joined together and open-circuit failures occur when a closed circuit is accidentally opened. The same study concludes that short-circuit failures have a significant voltage drop at the output, but also states that open circuit failures and degradation cause a significant decrease in current intensity.

A short-circuit failure can affect cells, bypass diodes, or PV modules. It is mainly due to water infiltration into the modules or poor wiring between the module and the inverter. In addition, the aging of photovoltaic modules, which is caused by the long-term operation of the PV, is one of the main sources of short-circuit failures. An open-circuit failure can occur if any current route that is serial to the load is accidentally removed or opened from a closed circuit. Such a situation occurs mainly due to an interruption in the cables between photovoltaic modules or solar cells (Garoudja et al., 2017). These relationships are fundamental to the design of the proposed methodology based on the model described below.

GPV modeling

There are several models for predicting the power output of a module, a chain of PV modules, or an array under certain conditions. Most of these models are based on voltage-current (I-V) ratios resulting from simplifications applied to the dual diode model (Tian et al., 2012): (1) 7-parameter model; (2) 5-parameter model Sandia Arrangement Performance Model (*SAPM);* (3) King model; (4) Equations of Luft and others; (5) Equations of Hadj Arab and others. Most of these models have the disadvantage that they require iterative methods and idealization values to match I-V curves to that of a specific cell or module; in addition to requiring experimental data that is not found in the manufacturer's data sheets. Taking into account the above the model selected to simulate the behavior of the GPV is the five-parameter model, popularized by (De Soto et al., 2006) since, unlike the other models, it only

ISSN: 2716-3865 (Print), 2721-1290 (Online)

requires information provided by the manufacturers and has been shown to match experimental results. It requires numerical methods of solution of systems of equations (De Soto et al., 2006). The behavior of a photovoltaic module can be modeled from the next equivalent circuit, known as a diode model, Figure 6, (Duffie and Beckman, 2013). This circuit includes a serial resistor (Rs) and a parallel diode with a resistor (R_p).

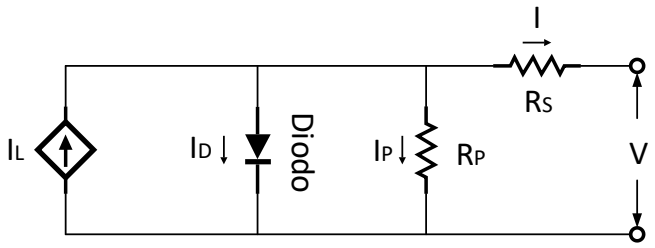

Figure 6. Equivalent circuit of a photovoltaic cell according to the 5PM model

To determine the voltage (V) and the current (I), five parameters must be known, which are (De Soto et al., 2006): (1) The photogenerated current (I_L); (2) The reverse saturation current of the diode (I_0); (3) The serial resistor (R_S); (4) Parallel Resistance (R_P); (5) The modified ideality factor (a).

The resulting current and voltage model determines the current and voltage given the solar cell parameters (Garoudja, 2017) as follows:

$$I=I_L-I_0\left[e^{\frac{V+IR_S}{a}}-1\right]-\frac{V+IR_S}{R_P} \qquad (1)$$

The simulation of a PV Generator consists of two stages shown below: Stage 1. Removing parameters in Standard Measurement Conditions: Irradiance of 1000W/m^2 and Operating Temperature of 25 ^oC. Equation 1, depends on the values of the five unknown parameters. These parameters are not provided in the manufacturer's data sheet, so accurate estimation of these parameters is an important step in GPV modeling. The method described by (De Soto et al., 2006) has been used to find these values. The data are under STC, with the exception of the NOCT variable, which is given by nominal operating conditions, irradiance of 800 W/m^2.

Stage 2. Determination of parameters under changes in operating conditions. From obtaining the five parameters in the STC, and taking into account the mathematical relationships of these parameters with environmental conditions (De Soto et al., 2006), it is possible to estimate the five parameters for the actual operating conditions and simulate the behavior of the GPV in any scenario.

Photovoltaic Generator Simulation

The simulations were performed based on the programming of the equations of the mathematical model of the GPV, using the professional software MATLAB 2017b. From the electrical parameters (Datasheet) of a commercial PV module HELIENE, model HEE215MA68, the mathematical model was parameterized allowing the simulation of the GPV for any environmental condition. Table 2 shows the main characteristics of this module.

Table 2. Main electrical parameters of the FV module

Electrical Data SCT	
Nominal Power PMPP (W)	250
Tension MPP (V)	30,30

ISSN: 2716-3865 (Print), 2721-1290 (Online)

Intensity MPP (A)	8,22
Vacuum tensión (V)	37,40
Short circuit current (A)	8,72

Figure 7, shows the behavior of the I-V curve against different irradiance values (*200* $\frac{W}{m^2}$ a *1000* $\frac{W}{m^2}$), keeping the operating temperature at 25 ^oC. The influence of irradiance has on photogenerated current and maximum power is evident, as the irradiance value increases, the short-circuit current and maximum power grow proportionally and vice versa. An open circuit voltage variation for different irradiance levels can also be shown, although it can be considered small compared to current variation.

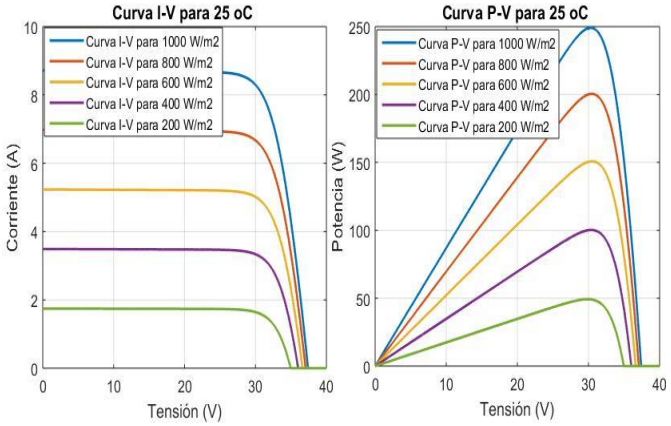

Figure 7. Simulation of the I-V behavior of the PV HELIENE module for changes in irradiance

Figure 8 shows the behaviour of the I-V curve against different operating temperature values (25 ^oC to 65 ^oC), maintaining irradiance in *1000* $\frac{W}{m^2}$. It is appreciated that the most dominant effect of temperature on the I-V curve focuses on the open circuit voltage, as the temperature value increases, the open circuit voltage and the maximum power decrease proportionally and vice versa.

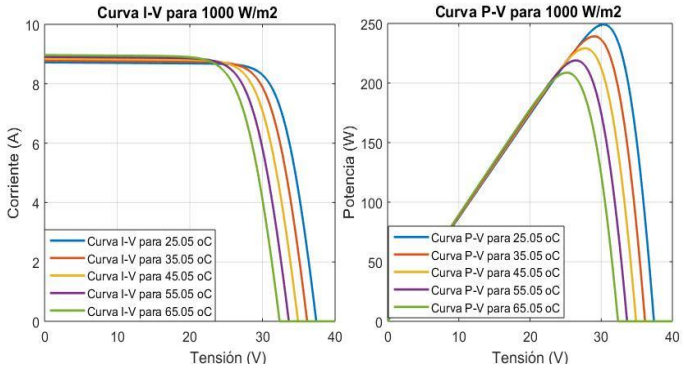

Figure 8. Simulation of the I-V behavior of a HELIENE FV module for changes in operating temperature

It can also be shown that the short-circuit current increases slightly for higher temperature values because the energy band, Band Gap, of the material decreases slightly with temperature as greater electron movement is created. It is shown that irradiance and temperature are the most important environmental variations and that open circuit tension and short-circuit current are essential for determining the actual behavior of an SPVGC. This will be used in the proposed methodology.

ISSN: 2716-3865 (Print), 2721-1290 (Online)

Procedure for quantifying operational losses of the GPV.

It should be known that for a correct design of a DDF system based on analytical redundancy it is necessary to have a model that describes the actual behavior of the system. For the GPV the model describes the system for ideal conditions, that is, depending on the nominal parameters provided by the manufacturer in its data sheet. However, the actual operation of the system takes into account operational losses, so accurate quantification of these losses is necessary in order to calibrate the GPV model to the actual operating conditions, avoiding false alarms due to a failure.

The analysis that is performed considers that the behavior of a photovoltaic system results from its instantaneous response to variations of two environmental conditions: the incident irradiance (S) and the operating temperature of the solar cells (Tc). In an ideal system, generating in low voltage and in the absence of shadows, the answer is given by the equations in Figure 9.

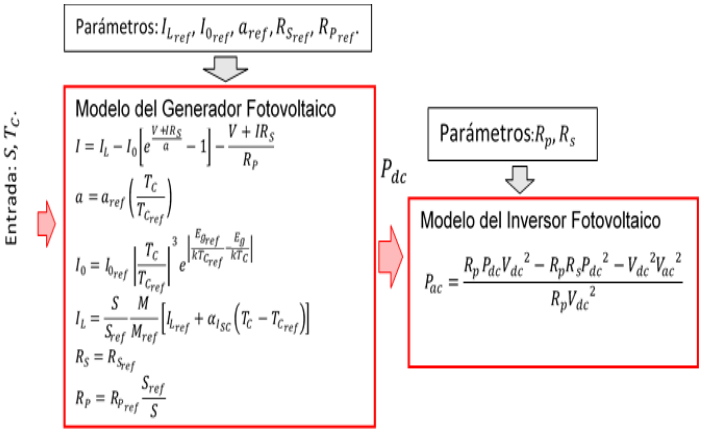

Figure 9: System of equations that define the GPV

Once the prevailing climate and the nominal parameters of the photovoltaic system have been characterized, it is possible to predict the behavior of the system and calculate the deviation between the ideal and real response (Lorenzo, 2007). The procedure for quantifying operational losses consists of Measure the system's power response to irradiance and cell temperature conditions for long enough to sweep the entire spectrum of operating conditions. The records obtained constitute a family of points in space (S, T_c, $P_{ac,EXP}$), that is, an experimental power value measured by $Pac,_{EXP}$ for each of the value pairs (S, Tc) that were presented during the test.

Calculate the power response that the system would have had if it had behaved exactly as described in the loss scenario set at the time of prediction. This leads to having a family of points in space (S, Tc, Pac,SIM) where Pac,SIM represents the calculated power values for the same pairs of values (S, Tc) that were presented during the trial (Lorenzo, 2007).

Determine the coefficient to be based on a polynomial adjustment of the shape $P_{ac,EXP}=(a)P_{ac,SIM}$ in which "a" represents the operational losses of the system under evaluation, that is, $P_{ope}=100\%*(1-a)$.

To achieve greater accuracy in model calibration, the potential required by the model-based fault diagnostic strategy described below, the operation data is adjusted to the coefficients a, b and c of polynomials:

$P_{dc,EXP}=(a_{Pdc}+b_{Pdc}(T_C\text{-}25°C)+c_{Pdc}S)P_{dc,SIM}$ (2) being $a_{P}dc$ in the value defined by the line $P_{dc,EXP}=(a_{Pdc})P_{dc,SIM}$

ISSN: 2716-3865 (Print), 2721-1290 (Online)

$V_{dc,EXP}=(a_{Vdc}+b_{Vdc}(T_C\text{-}25°C))V_{dc,SIM}$ (3) being a_{Vdc} in the value defined by the line $V_{dc,EXP}=(a_{Vdc})V_{dc,SIM}$

$I_{dc,EXP}=(a_{Idc}+b_{Idc}(T_C\text{-}25°C))I_{dc,SIM}$ (4) being a_{Idc} in the value defined by the line $I_{dc,EXP}=(a_{Idc})I_{dc,SIM}$

Where:

S is Irradiance, expressed in $\frac{W}{m^2}$.

T_C is the operating temperature of the PV module, expressed in ºC.

$P_{dc,EXP}$, $P_{dc,SIM}$ is the output power of the GPV measured and simulated respectively, expressed in W.

$V_{dc,EXP}$, $V_{dc,SIM}$ is the output voltage of the GPV measured and simulated respectively, expressed in V.

$I_{dc,EXP}$, $I_{dc,SIM}$ is the output current of the GFV measured and simulated respectively, expressed in A.

$P_{ac,EXP}$, $P_{ac,SIM}$ is the output power of the SPVGC measured and simulated respectively, expressed in W.

Obviously, if, P_{ope} turns out to be a positive term then the system does not meet the manufacturer's expectations, or has a certain level of exploitation. On the other hand, if P_{ope} is a negative term then the actual system response exceeds the results expected by the manufacturer. The importance of this conclusion lies in the verification of the warranty conditions of the PV modules.

Implementation of the procedure for quantifying operational losses in the 7.5 kWp FV SERC system

The test was carried out on the Photovoltaic Microsystem installed in the SERC throughout The month of June 2018. Experimentally obtained 8468 points in space 8468 puntos en el espacio (S, T_C, $P_{ac,EXP}$) and its correlatives were calculated in space (S, T_C, $P_{ac,SIM}$), Figure 10.

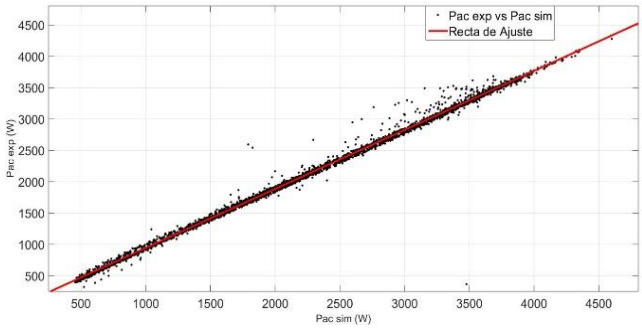

Figure 10. Result of the analysis of the operation data. Fit of the straight

The adjustment value was a=0.942 with a coefficient of determination for the straight, R^2=0.9951, therefore the operational losses of the system are P_{ope}=100%*(1-0.94)=6 %. A value of R^2 near the unit indicates that virtually all, 99.51%, of the variation of the observed result throughout the test is explained by the equation $P_{ac,EXP}=(0.94)*P_{ac,SIM}$.

The results obtained as part of the implementation of the procedure show that the critically evaluated PV Microsystem has power generation deficiencies, as operational losses amount to 6% with respect to the values expected by the manufacturer, in other words, the system operates at 94% of the nominal efficiency declared by the manufacturer for real environmental

ISSN: 2716-3865 (Print), 2721-1290 (Online)

conditions. Dissimilar causes may have an effect on this result such as: deviation of rated power in STC or degradation, DC wiring, among others. The values for adjusting the parameters of polynomials for calibration of the GPV mathematical model are shown in Table 3.

Table 3. Adjustment polynomial indexes

Polynomial	Parameters
Adjustment polynomial P_{dc}	a_{Pdc}=0.9411 b_{Pdc}=0.0772 %/℃ c_{Pdc}= -2.959*10^{-03} $\%/\frac{W}{m^2}$
Adjustment polynomial V_{dc}	a_{Vdc}=0.9941 b_{Vdc}=-0.000278 %/℃
Adjustment polynomial I_{dc}	a_{Idc}=0.9475 b_{Idc}=-3.47*10^{-03} %/℃

Figures 11 and 12 show the drawings defined by the mathematical model of the GPV calibrated from the polynomial described above with respect to experimental values.

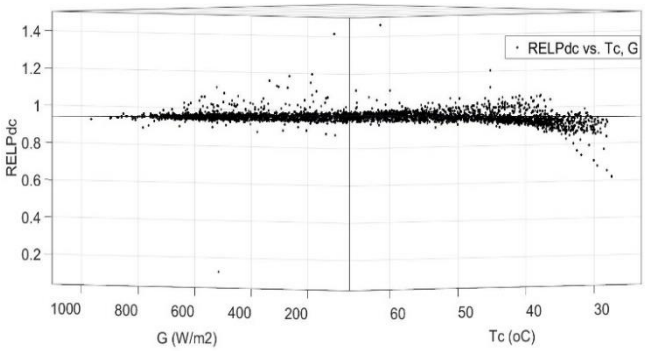

Figure 11. Theoretical plane of the maximum power point of the GPV with respect to the experimental data, front view

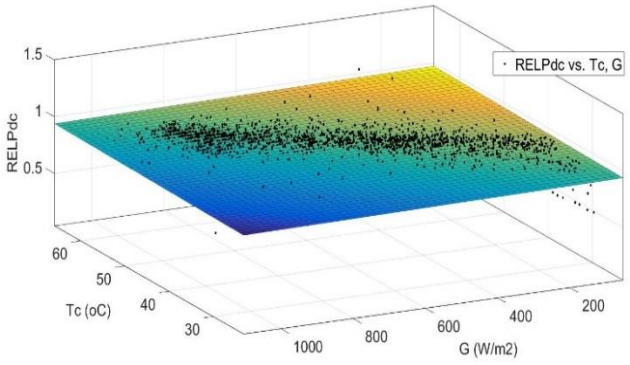

Figure 12. Theoretical plane of the maximum power point of the GPV with respect to the experimental data, diagonal view

Once operational losses have been quantified, it is necessary to design a fault diagnostic strategy that allows the detection and identification of failures that enables the management of greater efficiency through maintenance actions to the system.

Fault Diagnosis Strategy for SPVGC

Traditionally in manufacturing industries statistical quality control is used to monitor and control product quality. In addition, process control statistical charts can provide early

ISSN: 2716-3865 (Print), 2721-1290 (Online)

warnings of abnormal changes in system operations, which help operators identify the occurrence of potential failures, such as short circuits, circuits open, sensor polarization, among others (Garoudja *et al*., 2017).

gThese statistical tables include Shewhart, Cumulative Sum (CUSUM), and Exponentially Weighted Moving Average (EWMA) charts. Univariate statistical methods, such as the Shewhart and EWMA graphs, have been widely used to monitor industrial processes for many years (Montgomery, 2009). From here the EWMA was selected for this work.

EWMA-based DDF System Architecture for SPVGC

Once the mathematical model of the system in question has been developed and validated, a polynomial to fit the model to the actual operation data and taking advantage of the EWMA control charts is possible, it is possible to estimate the residuals, appearance important in model-based DDF systems. A residue, by definition, is only the difference between the value of the actual system and the simulated one from a mathematical model:

$$r(k)=y(k)-\hat{y}(k) \quad (5)$$

Where:

r(k). It's the residue at the moment k.

y(k). It's the actual exit of the system in the instant k.

$\hat{y}$(k). It's the output estimated by the model instant k.

The EWMA control chart is applied to monitor the residuals obtained from the DDF system. The upper and lower control limits of the EWMA chart for detecting an average change are:

$$NI/NS = \mu_0 \pm L\sigma_{z_t} \quad (6)$$

Where L is a multiplier of the standard deviation of EWMA σ_{z_t}. The parameters L y λ must be carefully defined. In general, L is specified in practice as 3, which corresponds to a false alarm rate of 0.27%, implying that 99.73% of observations must be within normal control limits under normal conditions (Garoudja, 2017).

The residues used, based on the characteristics of the monitoring system, as well as the advantages it provides in terms of the simplification of diagnostic analysis, are of the structured type. The design procedure consists of two steps: the first is to specify the sensitivity and insensitivity relationships between the residues and failures according to the assigned insulation task; secondly, a set of waste generators are designed that depend on the specified sensitivity and insensitivity ratios (Villegas Berbesi, 2012).

Sensitivity analysis is based on the classification of failures that occur on the DC side of an SPVGC. Short-circuits exhibit a significant voltage drop, so the variable sensitive to this type of failure is the voltage at the output of the GPV, this being a good indicator of identification of this type of failure. Depending on the magnitude of the short-circuit failure will be the number of PV modules in failure condition. On the other hand, open circuit failures have a significant current drop, so the variable sensitive to this type of failure is the output current of the GPV. On the other hand, the maximum power, being affected by both types of failures is a good indicator for the detection of these.

From this analysis, the residues were defined:

$$RI=\frac{I_{mpp\ real}-\left(a_{Idc}+b_{Idc}(T_C-25°C)\right)I_{mpp\ sim}}{\left(a_{Idc}+b_{Idc}(T_C-25°C)\right)I_{mpp\ sim}} \quad (7)$$

ISSN: 2716-3865 (Print), 2721-1290 (Online)

$$RV=\frac{V_{mpp\ real}-\left(a_{Vdc}+b_{Vdc}(T_C-25°C)\right)V_{mpp\ sim}}{\left(a_{Vdc}+b_{Vdc}(T_C-25°C)\right)V_{mpp\ sim}} \quad (8)$$

$$RP=\frac{P_{mpp\ real}-(a_{Pdc}+b_{Pdc}(T_C-25°C)+c_{Pdc}S)P_{mpp\ sim}}{(a_{Pdc}+b_{Pdc}(T_C-25°C)+c_{Pdc}S)P_{mpp\ sim}} \quad (9)$$

Where:

$I_{mpp\ real}$ y $I_{mpp\ sim}$ are the current values in PMP measured and simulated respectively.
$V_{mpp\ real}$ y $V_{mpp\ sim}$ are the voltage values in measured and simulated PMP respectively.
$P_{mpp\ real}$ y $P_{mpp\ sim}$ are the power values in PMP measured and simulated respectively.
a_{Idc}; b_{Idc}; a_{Vdc}; b_{Vdc}; a_{Pdc}; b_{Pdc} y c_{Pdc} are the coefficients of the adjustment polynomials of each of the variables.
S y T_C Irradiance and the operating temperature of the PV module respectively.

Knowing the form of connection of the GPV can be determined approximately how much a module or a PV chain represents in the monitored variables, so that these residues allow, from their magnitude, to determine the number of modules or chain of PV modules that are out of normal operation as they are defined as losses in percentage to the output of the mathematical model.

SPVGC fault identification algorithm

The proposed strategy starts from the maximum power to detect a failure. This choice is mainly due to the fact that failures inevitably affect this variable. Therefore, the maximum power is used as a fault indicator at the detection stage.

On the other hand, both the current and the DC voltage are not suitable to be used as sensitive indicators at this stage. For example, when a short circuit occurs in a photovoltaic module of a chain, the value of the current indicator will not change significantly from its set point in normal operation. In the meantime, a substantial change will appear in the maximum power indicator. In addition, the same situation occurs when a string is completely disconnected. In this case, the DC output voltage remains unchanged relative to its normal state as opposed to the maximum power, which if it decreases considerably (Garoudja et al., 2017).

However, in the isolation stage, current and voltage indicators if they have relevance, on the one hand, a short-circuit module mainly affects the voltage indicator while on the other hand an open circuit failure in a chain affects mainly the current indicator. Table 4, shows the fault signature matrix, result of system discoverability/isolability analysis.

Table 4. GPV fault signature matrix

	Normal Operation	Short-circuit failures			Open circuit failure
Residues	Normal	F1	F2	F3	F4
RP $\in$ [NI_{RP} NS_{RP}]	**1**	0	0	0	0
RV $\in$ [$NI_{RV} - \mathbf{0.1}$ $NS_{RV} - \mathbf{0.1}$]	0	**1**	0	0	0
RV $\in$ [$NI_{RV} - \mathbf{0.2}$ $NS_{RV} - \mathbf{0.2}$]	0	0	**1**	0	0
RV $\in$ [$NI_{RV} - \mathbf{0.4}$ $NS_{RV} - \mathbf{0.4}$]	0	0	0	**1**	0
RI $\in$ [$NI_{RI} - \mathbf{0.5}$ $NS_{RI} - \mathbf{0.5}$]	0	0	0	0	**1**

ISSN: 2716-3865 (Print), 2721-1290 (Online)

DDF Methodology Results

The proposed DDF methodology was validated using operating data collected from the 7.5 kWp SPVGC installed at the SERC in Santiago de Cuba, see Section 2. Based on this data, the control limits within which the system must operate if it is free of failures were calculated.

To evaluate this methodology, two case studies involving different types of failures were carried out. In the first case study, it is assumed that the photovoltaic system contains one or more short-circuited photovoltaic modules. In the second case study it is considered an open-circuit photovoltaic chain.

Normal operating conditions

The calculation of the control limits, which define the good performance of the SPVGC, was based on an operating database in the period for the month of June 2018. The residues were obtained from the equations in section 5.1.

Table 5, shows the limits of the control of the wastes (RI, RV, and RP) obtained as part of the analysis of the operation data.

Table 5. SFVCR waste control limits

Observed variables	Control limits
RP residue P_{mpp}	NS=0.0498 NI=-0.0498
RV residue V_{mpp}	NS=0.0149 NI=-0.0149
RI residue I_{mpp}	NS=0.0545 NI=-0.0545

Figure 13 shows how RP is kept within control limits showing that the system is free of failures. Thus Figures 14 and 15 show how the RI and RV behavior is also kept within the range set for the system under normal operating condition.

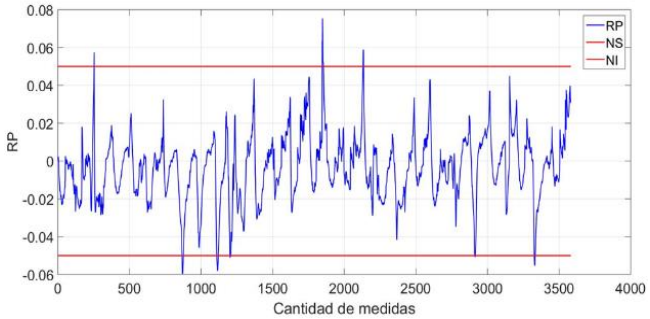

Figure 13. Result of RP waste monitoring for fault-free SPVGC

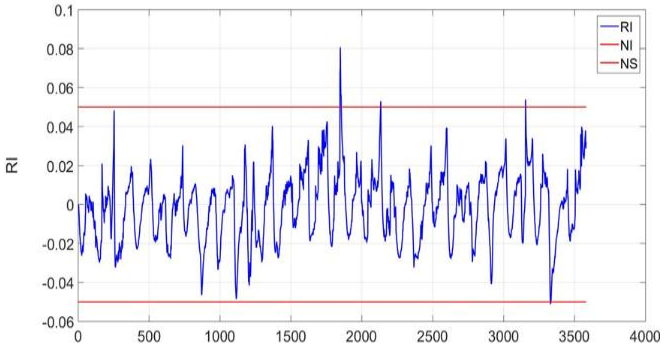

ISSN: 2716-3865 (Print), 2721-1290 (Online)

Figure 14. Result of RI residue monitoring for the fault-free SPVGC

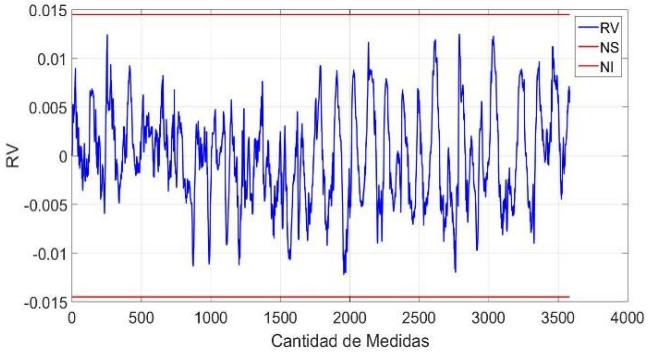

Figure 15. Result of RV residue monitoring for fault-free SPVGC

It is important to note that even though the system is in the normal operating condition, there are values of the residue that escape from the fault-free zone. Of the 3582 points obtained in the residue, the worst case has 8 points, corresponding to the RP residue, which are outside the range established in the normal operating condition, which is equivalent to a false alarm rate of 0.22%. This value implies that 99.78% of the observations are within the established range, demonstrating the quality of the proposed methodology when the system is in normal operating condition, in correspondence with what was raised in (Montgomery, 2009).

Short-circuit PV chain case study

In this case study, the behavior of the DDF algorithm is evaluated when a short-circuit failure occurs in PV modules. Three examples of failures are analyzed for this case: one short-circuit PV module, two short-circuit PV modules, and four short-circuit PV modules.

One short-circuit PV module

From the analysis of the data you can see that the DC current residues are within the control limits, i.e. this type of failure does not significantly affect this indicator. Not so for DC voltage residue than if it exhibits a deviation in correspondence with the control limits. Because a PV module is disconnected, a power equivalent to 10% of the rated power is lost, demonstrating the presence of a fault in that PV chain. Figure 16 shows when the fault is detected, and Figures 17 and 18 analyze the results related to the current and output voltage to identify the type of failure.

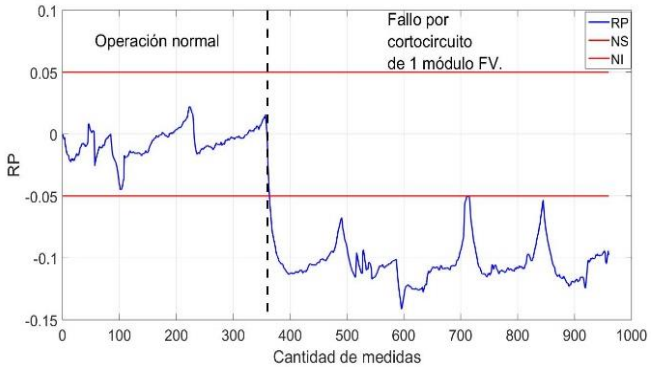

Figure 16. Result of Monitoring the EWMA control chart for RP residue in the presence of a short circuit failure in a PV module.

ISSN: 2716-3865 (Print), 2721-1290 (Online)

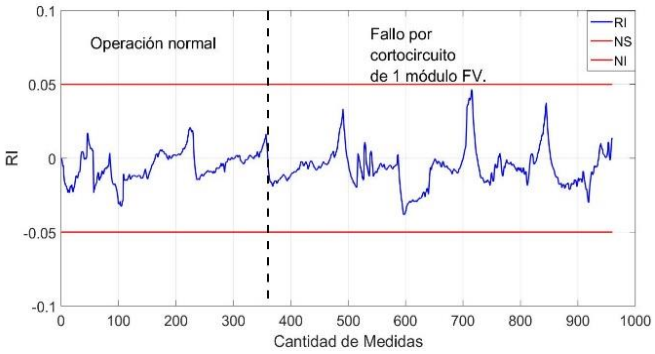

Figure 17. Result of Monitoring the EWMA control chart for RI residue in the presence of a short circuit failure in a PV module

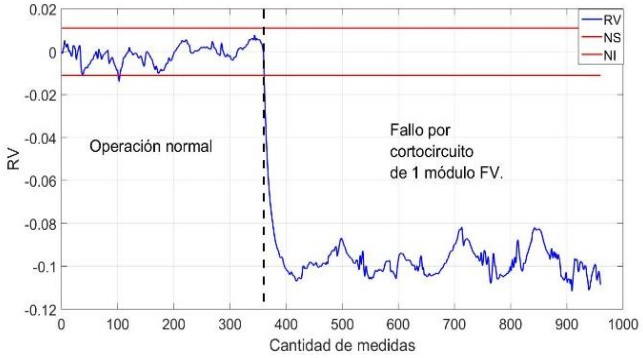

Figure 18. Result of Monitoring the EWMA control chart for RV residue in the presence of a short circuit failure in a PV module

According to the above algorithm a short circuit failure is identified as the current residue remains within the control limits while the voltage residue deviates from this range. According to the magnitude of the stress residue, it can be determined the number of PV modules that are in failure, taking into account that 10 modules are connected in series and the residue exhibits a drop of 10%, it is inferred that a module is in short failure in correspondence with the simulated failure.

Two short-circuit PV modules.

For this case the failure is simulated by disconnecting two modules from a FV chain. The behavior of the residuals is similar to the previous case, see Figure 19, because it is a failure of the same type, Figures 20 and 21.

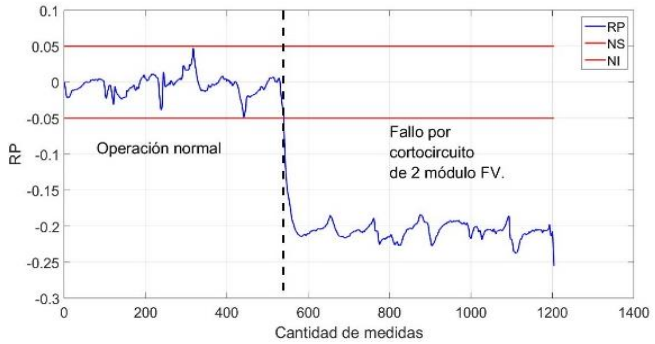

Figure 19. Result of Monitoring the EWMA control chart for RP residue in the presence of a short circuit failure in two PV modules

ISSN: 2716-3865 (Print), 2721-1290 (Online)

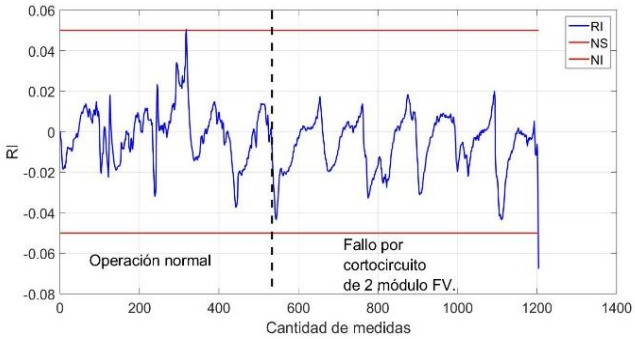

Figure 20. Result of Monitoring the EWMA control chart for RI residue in the presence of a short circuit failure in two PV modules

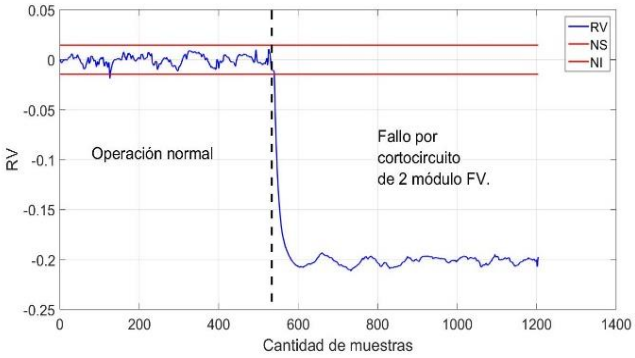

Figure 21. Result of Monitoring the EWMA control chart for RV residue in the presence of a short circuit failure in two PV modules

According to the magnitude of the stress residue it can be determined the number of PV modules that are in failure, taking into account that 10 modules are connected in series and the residue exhibits a drop of 20% is inferred that two modules are in short failure in correspondence with the simulated failure.

Four short-circuit PV modules

For this case the failure is simulated by disconnecting four modules from a FV chain. The behavior of the residuals is similar to the previous case, Figure 22, because it is a failure of the same type, Figures 23 and 24.

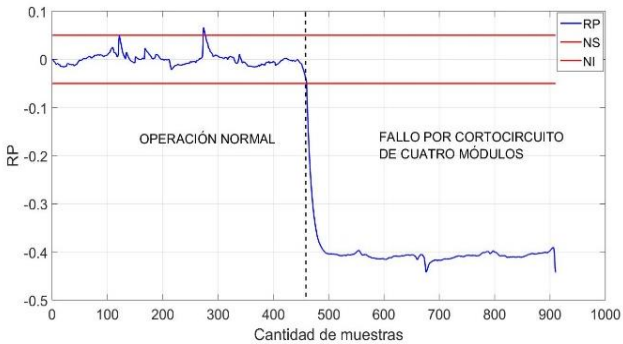

Figure 22. Result of Monitoring the EWMA control chart for RP residue in the presence of a short circuit failure in four PV modules

ISSN: 2716-3865 (Print), 2721-1290 (Online)

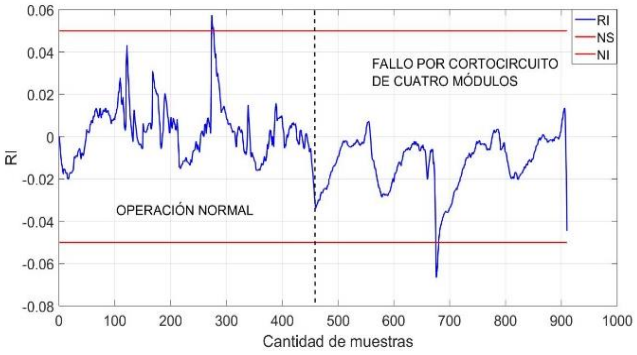

Figure 23. Result of Monitoring the EWMA control chart for RI residue in the presence of a short circuit failure in four PV modules

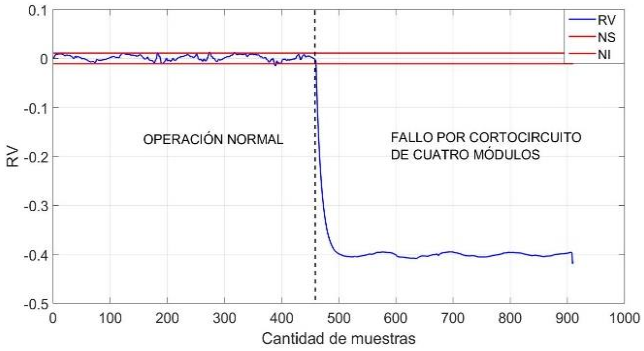

Figure 24. Result of Monitoring the EWMA control chart for RV residue in the presence of a short circuit failure in four PV modules

According to the magnitude of the stress residue, it can be determined the number of PV modules that are in failure, taking into account that 10 modules are connected in series and the residue exhibits a drop of 40% is inferred that four modules are faulty by cortocircuit in correspondence with the simulated failure.

Open-circuit PV chain case study

In this case, the performance of the proposed DDF algorithm is evaluated when an open circuit failure occurs. To do this, an open circuit failure is introduced into a PV array by disconnecting the second chain of the monitored PV system. Because one of the two chains of the PV array is disconnected, a large amount of power is lost, almost 50% of the rated power. After detecting the presence of the fault, Figure 25, the results related to the currenT and output voltage are analyzed to identify the type of fault, Figures 26 and 27.

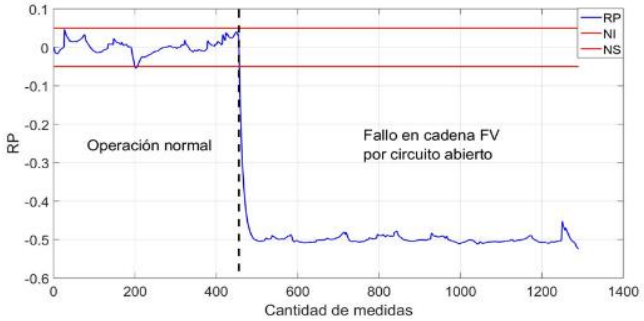

Figure 25. Result of Monitoring the EWMA control chart for RP residue in the presence of an open circuit failure

ISSN: 2716-3865 (Print), 2721-1290 (Online)

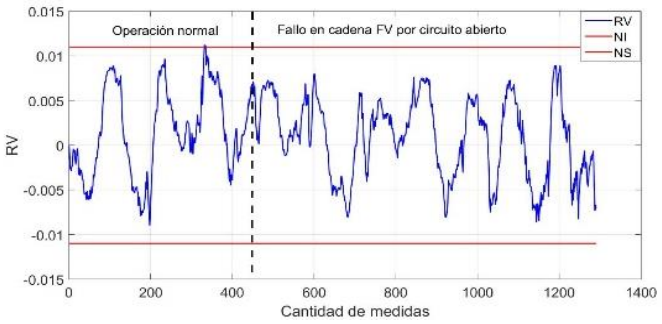

Figure 26. Result of Monitoring the EWMA control chart for RV waste in the presence of an open circuit failure

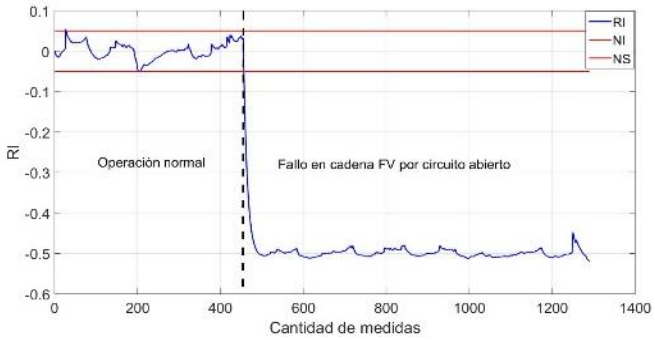

Figure 27. Result of Monitoring the EWMA control chart for RI residue in the presence of an open circuit failure

According to the proposed algorithm an open circuit failure is identified as the voltage residue remains within the control limits while the current residue deviates from this range. According to the magnitude of the current residue, the amount of PV chains that are in failure can be determined, considering that two chains are connected to the Inverter and the residue exhibits a 50% drop it is inferred that a chain is faulty by open circuit in correspondence with the simulated failure.

Conclusion

In model-based fault detection approaches, both solar irradiance and PV module temperature measurements are necessary to predict the maximum power point (MPP) of the SPVGC. A methodology was developed to monitor the performance of photovoltaic systems by detecting DC-side failures and diagnosing the type of failure detected. Due to the wide variety of failures that can occur in a GPV, a classification was used based on the electrical properties induced to the system when it is operating in fault condition: open circuit failures and short circuit failures. Voltage and current residues are used to differentiate between open circuit failures and short circuit failures in a photovoltaic system, and depending on the magnitude of the residue will be the amount of PV modules that are in failure condition. Using practical data from a 7.5 kWp SPVGC installed in the SERC, the methodology was able to detect and identify 100% of simulated failures and the tests performed had a maximum of a false alarm rate of 0.22%, demonstrating its capacity. The application of this methodology in SPVGC helps to raise indicators of efficiency, maintainability and availability by reducing the downtime, detection and repair of the modules.

References

Villegas Berbesi, T. (2012). Aplicación de técnicas robustas para detección y diagnóstico de fallos.

ISSN: 2716-3865 (Print), 2721-1290 (Online)

Brooks, B. (2011). The bakersfield fire: a lesson in ground-fault protection. *SolarPro Mag*, *62*.

Chouder, A., & Silvestre, S. (2009). Analysis model of mismatch power losses in PV systems. *Journal of Solar Energy Engineering*, *131*(2).

Chouder, A., & Silvestre, S. (2010). Automatic supervision and fault detection of PV systems based on power losses analysis. *Energy conversion and Management*, *51*(10), 1929-1937.

De Soto, W., Klein, S. A., & Beckman, W. A. (2006). Improvement and validation of a model for photovoltaic array performance. *Solar energy*, *80*(1), 78-88.

Duffie, J. A., & Beckman, W. A. (2013). *Solar engineering of thermal processes*. John Wiley & Sons.

Firth, S. (2006). *Raising efficiency in photovoltaic systems: high resolution monitoring and performance analysis* (Doctoral dissertation, De Montfort University).

Garoudja, E., Harrou, F., Sun, Y., Kara, K., Chouder, A., & Silvestre, S. (2017). Statistical fault detection in photovoltaic systems. *Solar Energy*, *150*, 485-499.

Houssein, A., Heraud, N., Souleiman, I., & Pellet, G. (2010, December). Monitoring and fault diagnosis of photovoltaic panels. In *2010 IEEE International Energy Conference* (pp. 389-394). IEEE.

Lorenzo, E., Martínez, F., Muñoz, J., & Fernández, L. N. (2007). Predicción y ensayo de la producción de energía fotovoltaica conectada a la red: retratos de la conexión fotovoltaica a la red (IX). *Era solar: Energías renovables*, (139), 22-31.

Mekki, H., Mellit, A., & Salhi, H. (2016). Artificial neural network-based modelling and fault detection of partial shaded photovoltaic modules. *Simulation Modelling Practice and Theory*, *67*, 1-13.

Meyer, E. L., & Van Dyk, E. E. (2004). Assessing the reliability and degradation of photovoltaic module performance parameters. *IEEE Transactions on reliability*, *53*(1), 83-92.

Montgomery, D. C. (2007). *Introduction to statistical quality control*. John Wiley & Sons.

Munoz, M. A., Alonso-García, M. C., Vela, N., & Chenlo, F. (2011). Early degradation of silicon PV modules and guaranty conditions. *Solar energy*, *85*(9), 2264-2274.

Gutiérrez, A. S., Eras, J. J. C., Hens, L., & Vandecasteele, C. (2017). The biomass based electricity generation potential of the province of Cienfuegos, Cuba. *Waste and Biomass Valorization*, *8*(6), 2075-2085.

Gutiérrez, A. S., Eras, J. J. C., Huisingh, D., Vandecasteele, C., & Hens, L. (2018). The current potential of low-carbon economy and biomass-based electricity in Cuba. The case of sugarcane, energy cane and marabu (Dichrostachys cinerea) as biomass sources. *Journal of Cleaner Production*, *172*, 2108-2122.

Stettler, S., Toggweiler, P., Wiemken, E., Heydenreich, W., De Keizer, A. C., van Sark, W. G. J. H. M., ... & Beyer, H. G. (2005, June). Failure detection routine for grid-connected PV systems as part of the PVSAT-2 project. In *Proceedings of the 20th European Photovoltaic Solar Energy Conference & Exhibition, Barcelona, Spain* (pp. 2490-2493).

ISSN: 2716-3865 (Print), 2721-1290 (Online)

Tian, H., Mancilla-David, F., Ellis, K., Muljadi, E., Jenkins, P., 2012. Detailed Performance Model for Photovoltaic Systems: Preprint. United States. National Renewable Energy Laboratory. 56 páginas.

Vergura, S., Acciani, G., Amoruso, V., & Patrono, G. (2008, June). Inferential statistics for monitoring and fault forecasting of PV plants. In *2008 IEEE International Symposium on Industrial Electronics* (pp. 2414-2419). IEEE.

Vergura, S., Acciani, G., Amoruso, V., Patrono, G. E., & Vacca, F. (2008). Descriptive and inferential statistics for supervising and monitoring the operation of PV plants. *IEEE Transactions on Industrial Electronics*, *56*(11), 4456-4464.

Zhao, Y., (2010). Fault analysis in solar photovoltaic arrays. Master's thesis, Northeastern University. Boston, Massachusetts. http://hdl.handle.net/2047/d20003009

Zhao, Y., Ball, R., Mosesian, J., de Palma, J. F., & Lehman, B. (2014). Graph-based semi-supervised learning for fault detection and classification in solar photovoltaic arrays. *IEEE Transactions on Power Electronics*, *30*(5), 2848-2858.

Zhao, Y., Lehman, B., Ball, R., Mosesian, J., & de Palma, J. F. (2013, March). Outlier detection rules for fault detection in solar photovoltaic arrays. In *2013 Twenty-Eighth Annual IEEE Applied Power Electronics Conference and Exposition (APEC)* (pp. 2913-2920). IEEE.

Zhao, Y., Yang, L., Lehman, B., de Palma, J. F., Mosesian, J., & Lyons, R. (2012, February). Decision tree-based fault detection and classification in solar photovoltaic arrays. In *2012 Twenty-Seventh Annual IEEE Applied Power Electronics Conference and Exposition (APEC)* (pp. 93-99). IEEE.

ISSN: 2716-3865 (Print), 2721-1290 (Online)